SCIENCE CHINA
Technological Sciences

• RESEARCH PAPER •

September 2025, Vol. 68, Iss. 9, 1920204:1–1920204:11
https://doi.org/10.1007/s11431-025-2997-0

Precision glass molding with high-temperature metallic glass as inserts

Fei SUN[1], Yuan HUANG[1], Sirui CHENG[4], Shike HUANG[2], Xichuan WANG[1], Jiahua ZHU[1], Wenfei LU[1], Ying DING[1], Tingting WU[1], Jiang MA[2*], Yanhui LIU[3*] & Jun SHEN[1*]

[1] *School of Materials Science and Engineering, Fujian University of Technology, Fuzhou 350118, China*
[2] *State Key Laboratory of Radio Frequency Heterogeneous Integration, Shenzhen University, Shenzhen 518060, China*
[3] *Institute of Physics, Chinese Academy of Sciences, Beijing 100190, China*
[4] *Beijing Machine and Equipment Institute, Beijing 100854, China*

Received April 15, 2025; accepted July 14, 2025; published online August 8, 2025

Abstract The microlens array (MLA) has been extensively utilized in optical systems; however, fabricating high-precision MLA molds for glass molding remains a significant challenge due to the inherent hardness and brittleness of conventional mold materials. In the present investigation, an Ir-Ni-Ta-Nb high-temperature metallic glass (ht-MG) is methodically examined as a promising alternative mold material for precision glass molding. The high-temperature properties of ht-MG—including compressive strength, hardness, oxidation resistance, thermal expansion, and adhesion resistance—are systematically evaluated, confirming its suitability for mold applications. Furthermore, utilizing the thermoplastic formability of ht-MG, MLA molds with a unit diameter of 80 μm and a sagittal height of 25 μm are successfully fabricated. Surface roughness measurements further confirmed the fidelity of the pattern transfer, with the ht-MG mold exhibiting only a slight increase in roughness from 4.583 to 4.735 nm, whereas the final glass MLA maintains a surface roughness of 5.689 nm. The glass MLA fabricated via the ht-MG mold exhibits an exceptional replication rate of 99.5%, ensuring fairly accurate structural reproduction. Furthermore, optical characterization confirms that the molded glass MLA possesses high-quality imaging and focusing capabilities, with well-defined focal spots and minimal aberrations. The uniformity of the microlenses and their optical performance firmly confirm the effectiveness of the ht-MG mold in achieving precise optical structures. This study effectively presents a reliable material and non-mechanical-machining strategy for fabricating high-precision MLA molds via amorphous alloy materials and provides an effective scalable approach for manufacturing high-performance optical glass components.

Keywords microlens array, precision glass molding, optical molds, high-temperature metallic glass

Citation: Sun F, Huang Y, Cheng S R, et al. Precision glass molding with high-temperature metallic glass as inserts. Sci China Tech Sci, 2025, 68(9): 1920204, https://doi.org/10.1007/s11431-025-2997-0

1 Introduction

Microlens arrays (MLA) possess excellent light manipulation capabilities and versatile design flexibility, making them essential optical components for a wide range of applications, including optical sensing, communication systems, and advanced digital displays [1–4]. Optical glass and plastics are commonly used as primary materials in the manufacturing of MLA products [5]. Compared with plastics, optical glass offers higher mechanical strength, better optical performance, lower thermal expansion, and greater environmental stability, making it an optimal choice for applications that require precision, reliability, and long-term durability [6]. Nevertheless, precision fabrication of microstructures on glass remains a major challenge due to its inherent hardness and brittleness, which severely limit the feasibility of conventional machining techniques [7]. Although advanced non-conventional machining techniques, such as single-point diamond cutting, photolithography,

* Corresponding author (email: majiang@szu.edu.cn; yanhui.liu@iphy.ac.cn; junshen@fjut.edu.cn)

ultrafast laser ablation, and focused ion beam (FIB) milling, allow the fabrication of microscopic optical structures on glass, they are often costly, labor-intensive, and impractical for scalable manufacturing [8–11]. As a result, cost-effective, high-precision, and scalable processing techniques for precision glass MLA are highly demanded in advanced optics and photonics.

Taking advantage of the thermoplastic formability of glass, precision glass molding (PGM) has been considered a promising route for efficient and high-precision fabrication of glass MLA components [12–14]. Notably, the adoption of PGM requires mold materials with exceptional high-temperature performance and superior machinability [15]. Typical mold materials include tungsten carbide (WC) and silicon carbide (SiC). They are utilized due to their superior mechanical properties, low thermal expansion coefficient, and strong adhesion resistance [16,17]. Although they are suitable for the fabrication of macroscale optical structures, it is challenging to create micro-/nano-array structures on these materials due to their high hardness and brittleness. Electroformed nickel and its alloys, which enable the fabrication of micron-sized structures and nanoscale surface roughness, are alternative candidates for mold materials. However, their environmental unfriendliness and poor high-temperature tolerance limit their applications [18,19]. Silicon (Si) has been used for micron-/nano-scale glass molding. However, its susceptibility to wear at elevated temperatures and severe adhesion to glass prevent them from being used for PGM. With the growing demand for glass optical components with smaller unit sizes and higher quality, the development of mold materials with high-temperature durability and superior machinability has become increasingly crucial for advanced PGM processes [20].

Metallic glasses (MGs) represent an advanced class of metallic materials characterized by the absence of defects such as dislocations and grain boundaries. They exhibit outstanding properties, including high strength, superior hardness, and excellent wear resistance [21–23]. Notably, MGs can be thermoplastically processed when heated into the supercooled liquid region (SLR), and complex surface structures with precise geometries at the macro, micro-/nano-scales can be obtained [24–27]. The unique characteristics of MGs provide a cost-effective and convenient way to precisely fabricate micro-optical structures, making them a highly promising material for PGM molds. Unfortunately, most existing MGs exhibit low glass transition temperatures ($T_g \leqslant 500$°C) or narrow SLRs (ΔT) for effective thermoplastic processing. To date, direct applications of MGs as an optical mold in glass molding have rarely been reported.

In our previous work, we developed an Ir-Ni-Ta-Nb high-temperature MG with a high glass transition temperature ($T_g \approx 827$°C), a wide ΔT ($T_x - T_g \approx 128$°C), and an excellent high-temperature wear resistance, demonstrating significant potential for PGM [28]. Compared to Zr-based and Pt-based MGs, the Ir-Ni-Ta-Nb high-temperature metallic glass (ht-MG) developed in this study offers a higher glass transition temperature and superior oxidation resistance at elevated temperatures. These features enable its stable performance during repeated high-temperature molding processes, which is essential for reliable and long-term use in precision optical component fabrication. In the current investigation, we propose a practical, non-mechanical-machining strategy for fabricating precise MLA molds with the ht-MG having high strength, small thermal expansion, and oxidation and adhesion resistance. Through thermoplastic forming (TPF), an MLA structure (80 μm diameter, 25 μm height) was precisely created on the surface of ht-MG by replicating a commercial Si template. The fabricated MLA mold achieved a replication rate of 98.4%, demonstrating high structural accuracy and minimal form deviation during the TPF process. Surface roughness analysis further confirmed the excellent pattern fidelity. The ht-MG mold was used to fabricate glass MLA by PMG. Imaging and focusing experiments indicate that the glass MLA exhibits excellent optical performance, suggesting that the ht-MG is a reliable material as MLA mold and the fabrication strategy for ht-MG molds is effective and suitable for scalable PGM.

2 Experimental

2.1 Materials preparation

Ht-MG with a nominal composition of $Ir_{29.8}Ta_{34.6}Ni_{29.3}Nb_{6.3}$ was fabricated by copper mold casting. As illustrated in Figure 1(a), the master alloy was prepared by arc melting an elemental mixture with a purity of at least 99.9% in a Ti-purged argon atmosphere. Each ingot was remelted five times to ensure compositional homogeneity. By casting the molten alloy into a water-cooled copper mold for rapid cooling, plate-like ht-MGs of dimensions of 1.2 mm × 12 mm × 15 mm were methodically obtained. The plate-like ht-MGs were then cut into 10 mm-diameter discs (see Figure 1(b)) via low-speed wire electrical discharge machining (WEDM; SODICK AP250L). Before the TPF process, all samples were polished to a mirror finish. The MLA-patterned Si templates, with lens unit diameters of 80 μm and sag heights of 25 μm, were purchased from commercial suppliers and served as precursor templates for thermoforming MLA structures onto the ht-MG's surface. In addition, a 500 nm-thick Si_3N_4 coating was deposited on the surface of the Si template using plasma-enhanced chemical vapor deposition (PECVD) to enhance the high-temperature strength. The deposition process was carried out in a vacuum environment with a pressure better than 4.0×10^{-5} Pa at 220°C. The gas flow ratio was SiH_4:NH_3:N_2 = 6:22:72, and the deposition time was 60 min. The deposition power was

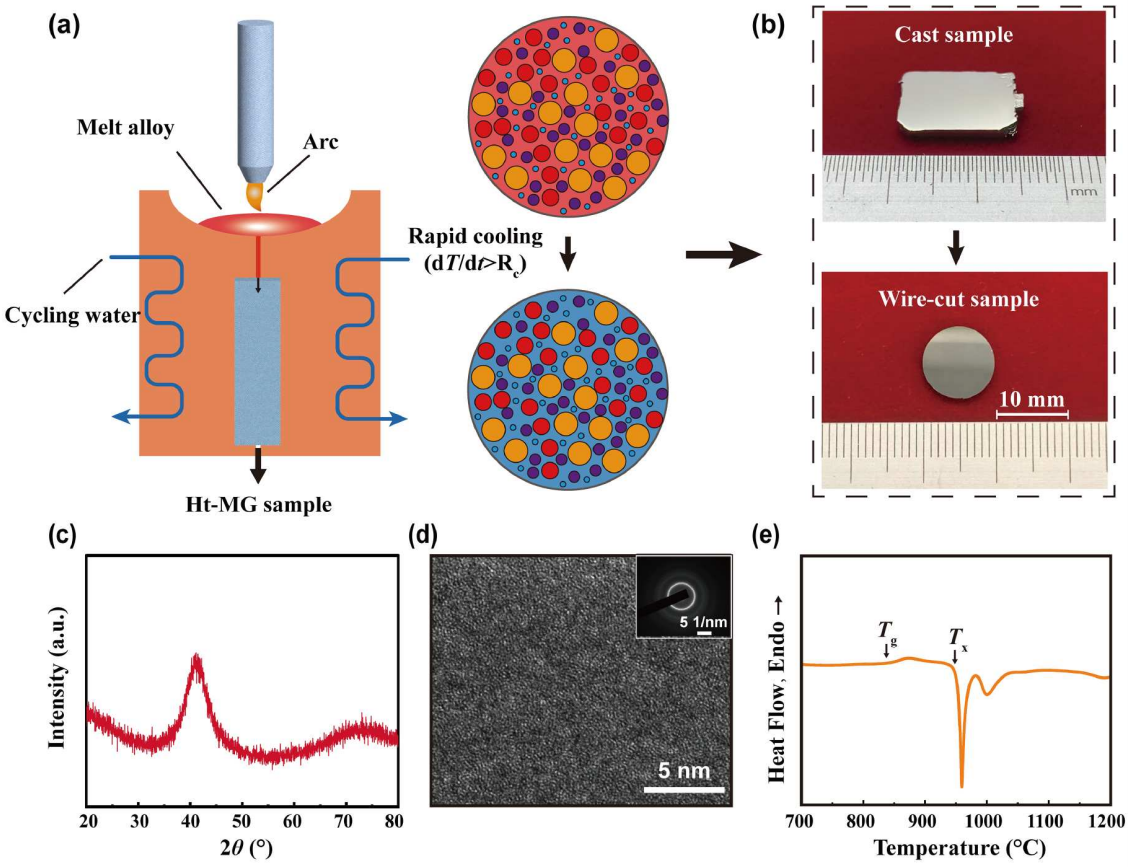

Figure 1 (Color online) (a) Schematic of ht-MG fabrication via copper mold casting; (b) typical cast and wire-cut samples; (c)–(e) XRD, TEM, and DSC results of ht-MG.

100 W, and the electrode spacing was 20 mm. Cemented carbide (92 wt.% WC, 8 wt.% Co) and 6H-SiC were selected as reference materials for the anti-adhesion test. The glass billets utilized for the anti-adhesion test have a diameter of 4 mm and a height of 5 mm, while those employed for the PGM process have a diameter of 10 mm and a thickness of 2 mm. The optical glass used for the adhesion and molding tests is specified as D-K59 (CDGM Glass Co., Ltd., China). It has a T_g of 497°C and a softening point (T_s) of 551°C, with a density of 2.41 g/cm^3, a Poisson's ratio of 0.212, and a Young's modulus of 8303×10^7 Pa.

2.2 Characterizations

The glassy nature of the ht-MG samples was mainly characterized by X-ray diffraction (XRD; Rigaku MiniFlex 600) with Cu Kα radiation and transmission electron microscopy (TEM; JEM-2100F). The thermal properties were measured using high-temperature differential scanning calorimetry (DSC, NETZSCH 404 F1) at a heating rate of 20°C/min. The high-temperature mechanical properties of ht-MG and the deformation behavior within the SLR were also tested via a universal material testing machine (Instron 5500). In addition, the high-temperature hardness of ht-MG was tested via a Hugetall-type Vickers hardness tester. A Thermo Mechanical Analyzer (TMA, NETZSCH 402 F1) and a Thermogravimetric Analyzer (TG, NETZSCH 209F3) were used to assess the oxidation resistance and thermal expansion properties of ht-MG, respectively. The anti-adhesion properties between ht-MG and molten glass were evaluated using a high-temperature contact angle (HCA) meter (OCA25-HTV1800). The three-dimensional (3D) morphology and dimensional accuracy of the MLA molds, as well as the glass components, were appropriately evaluated using a field emission scanning electron microscope (SEM; FEI QUANTA FEG 450) and a laser confocal microscope (LEXT OLS5100). Further, the surface roughness was measured via atomic force microscopy (AFM, OXFORD MFP-3D Infinity).

2.3 Thermoforming equipment and process

The TPF of both ht-MG molds and optical glass elements was methodically carried out via self-developed equipment (TM-YJ-03, Shenzhen University, China). The system uses resistance heating and reaches a maximum temperature of

1200°C with an accuracy of ±2°C. The pressing mechanism relies on a closed-loop servo-cylinder that offers a load capacity of 0.1–30 kN with an accuracy of 0.01 kN. The machine reaches a vacuum level of 3×10^{-4} Pa and incorporates a circulating water-cooling system. The ht-MG thermoforming temperature was set as 900°C, whereas the PGM molding temperature was set equal to 520°C according to the thermodynamic properties of the selected optical glass. In addition, the pressure, loading rate, and holding time in order were set as 200 N, 0.01 mm/s, and 1 min. Further, the heating process was conducted at 30°C/min under a vacuum of 5×10^{-4} Pa.

3 Results and discussion

3.1 High-temperature performance of the ht-MG

Figure 1(c) presents the XRD pattern of the as-cast ht-MG sample, which exhibits a broad diffraction peak at about 42°, confirming its amorphous nature. Figure 1(d) displays the high-resolution TEM (HRTEM) image and selected area electron diffraction. The halo diffraction pattern further validates the fully amorphous structure at the atomic scale. The DSC curve of the ht-MG is presented in Figure 1(e). According to the curve, T_g and crystallization temperature (T_x) of the ht-MG are approximately 827°C and 955°C, respectively, comparable to those of the Ir-Ni-Ta-(B) MG system [29]. The high T_g and wide ΔT (i.e., $T_x - T_g \approx 128$°C) indicate excellent thermal stability and thermoplastic molding capabilities of the ht-MG. Notably, T_g of the ht-MG exceeds that of most low-to-medium-softening-point optical glasses ($\leqslant$ 700°C). This is the essential prerequisite for the precise fabrication of MLA molds suitable for glass molding [30].

Generally, mold materials suitable for PGM should essentially meet the following properties [31,32]: (1) excellent mechanical strength to endure repeated molding cycles at high temperatures; (2) high chemical stability to prevent oxidation and chemical interactions with glass; (3) low coefficient of thermal expansion to minimize dimensional deviations in optical elements due to thermal fluctuations. Therefore, to assess the suitability of ht-MG as a mold material for glass molding, its high-temperature properties, including compressive strength, hardness, oxidation resistance, and thermal expansion, are systematically evaluated.

Considering the T_g of most low-to-medium softening-point optical glasses ($T_g \leqslant$ 700°C), we evaluated the compressive strength and hardness at temperatures of room temperature (RT), 200°C, 400°C, 600°C, and 750°C, respectively. As presented in Figure 2(a), the ht-MG exhibits a high strength of approximately 3.34 GPa at RT. With the increase in temperature, the strength gradually decreases. In the temperature range of 400°C–600°C, where most low-softening-point optical glasses are molded, the strength of the ht-MG remains between 2.26 and 2.86 GPa. Even at 750°C, a high strength of 2.00 GPa can be maintained. These indicate that the strength meets the requirements for PGM [13,33]. The hardness of the ht-MG at high temperatures was measured via a Vickers hardness tester with a load of 1000 g and a holding time of 10 s. As shown in Figure 2(b), the hardness at RT is as high as 1224.2 HV. In the temperature range of 400°C–600°C, the hardness decreases from 1188.8 to 1135.7 HV. At 750°C, the ht-MG can maintain a high hardness of 1116.8 HV. In addition to mechanical properties, oxidation resistance is another critical property of mold materials, as it prevents aging and degradation, thereby enhancing durability. We measured the weight gain of ht-MG under a continuous flow of compressed air upon heating at a rate of 20°C/min. The results (Figure 2(c)) indicate that oxidation is ignorable up to ~630°C. This suggests the excellent resistance of the ht-MG to oxidative degradation at high temperatures. In addition, low thermal expansion is essential to minimize shape errors caused by thermal expansion and contraction during glass molding. We measured thermal expansion of the ht-MG from RT to 800°C under a positive pressure of 0.03 N, at a heating rate of 5°C/min. From Figure 2(d), one can see that the ht-MG exhibits a linear thermal expansion up to 745°C. The average thermal expansion coefficient is 7.1 ppm/K. It is noteworthy that the coefficient is among the smallest values compared with existing MGs [29,34]. The above results indicate that the ht-MG exhibits excellent high-temperature performance, making it an ideal mold material for PGM.

3.2 Adhesion of ht-MG to optical glass

Adhesion between the mold and optical glass is a critical issue in the PGM process. At temperatures above 500°C, the mold surfaces can become reactive and prone to adhering to chemically activated glass, which could drastically reduce the service time of the mold and degrade the quality of glass elements. Therefore, it is essential to evaluate the adhesion resistance at high temperatures. The measurement of the HCA between molten glass and the mold is widely recognized as an intuitive and effective approach for evaluating adhesion resistance [35–37]. In the present investigation, the HCA test was performed in an atmospheric environment to assess the adhesion between ht-MG and glass. For comparison, three typical mold materials—tungsten carbide (WC), silicon carbide (SiC), and silicon (Si) wafer—were also tested under identical conditions. All the materials were polished to a mirror surface before HCA tests. To ensure complete melting of the optical glass, the mold materials and glass were simultaneously heated to 850°C at a rate of 10°C/min. As presented in Figure 3(a), the glass starts to melt at 750°C and becomes fully molten at 800°C. At 800°C,

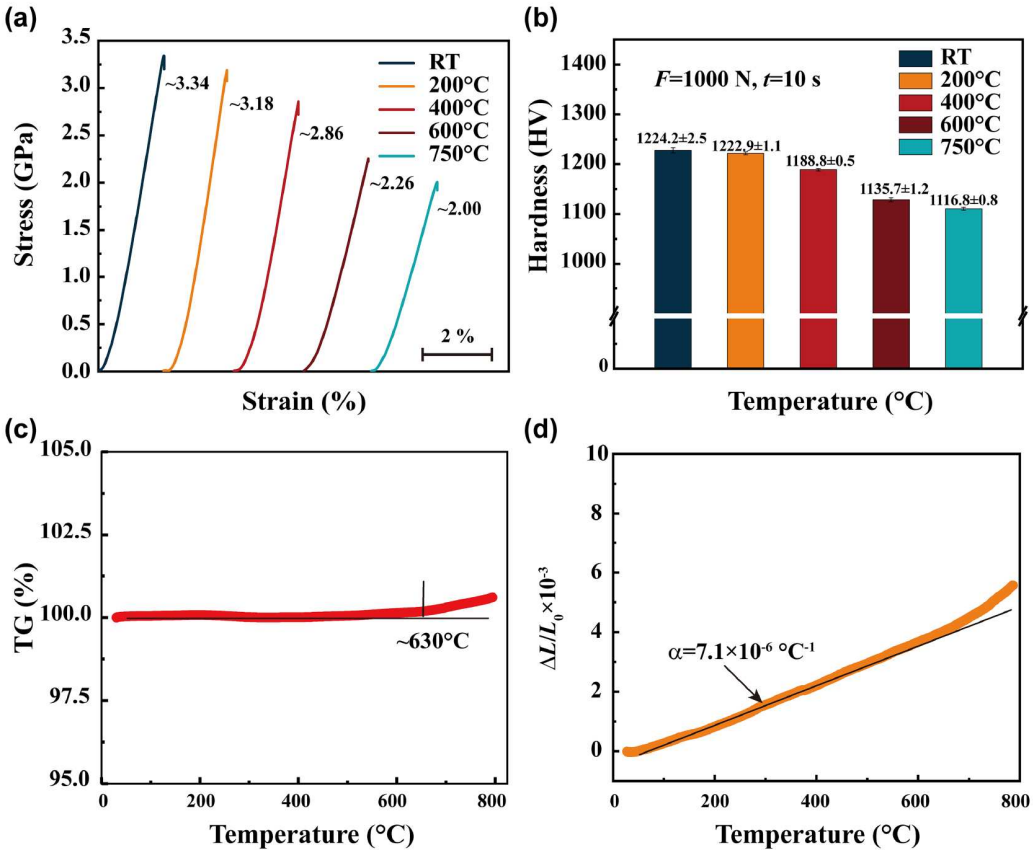

Figure 2 (Color online) (a), (b) The compressive strength and hardness of ht-MG at different temperatures; (c), (d) the oxidative weight gain and thermal expansion properties of ht-MG.

the HCA between ht-MG and molten glass is 142.1°, whereas the HCA for other mold materials is about 134°. This indicates that the ht-MG is better than typical mold materials in anti-adhesion properties. As the temperature increases to 850°C, the HCA for all the materials decreases. This is due to the increased chemical reactions between the optical glass and mold materials. Figure 3(b) presents a detailed comparison of the variation of temperature-dependent HCA between molten glass and mold materials in the range of 800°C to 850°C. It is observed that the HCA for ht-MG is the largest and ht-MG is the only material exhibiting HCA exceeding 140° between 800°C and 830°C. Within the test temperature range, ht-MG maintains the advantage of higher HCA, and thus superior anti-adhesion properties compared to conventional mold materials. The enhanced anti-adhesion behavior is attributed to the irregular atomic structure of ht-MG, which results in low surface energy, along with the intrinsic chemical inertness due to the presence of noble metal Ir [38]. The surface morphology of the mold materials after HCA testing is shown in Figure S1 (Supporting Information). It is worth mentioning that the glass on ht-MG, WC, and SiC can be easily removed. However, severe adhesion occurred on the Si surface. Furthermore, it was observed that all materials reacted with molten glass at 850°C, but the ht-MG only exhibited slight adhesion to optical glass, consistent with the HCA results.

Furthermore, we conducted a 10-cycle simulated PGM experiment at 520°C. The surface morphology of the mold materials was examined to evaluate the anti-adhesion properties of the ht-MGs. The experiment was conducted at a heating rate of 30°C/min under a vacuum of 5×10^{-4} Pa. When the temperature reached 520°C, a pressure of 100 N was applied for 1 min, followed by pressure release and furnace cooling. Si mold was not tested due to the severe adhesion to glass. As shown in Figure 4, only a small amount of glass debris can be observed on the ht-MG surface, while severe adhesion occurred on the WC and SiC surfaces. WC and SiC are produced via powder sintering, leading to micro-/nano-scale defects, such as pores and cracks. These defects are inevitably transferred to the glass surface during the PGM process, ultimately degrading its optical properties. In contrast, the superior surface quality of ht-MG offers substantial advantages as a molding mold, ensuring high precision and enhanced optical performance.

3.3 Fabrication of ht-MG molds and glass components

We next develop the strategy for mold fabrication using

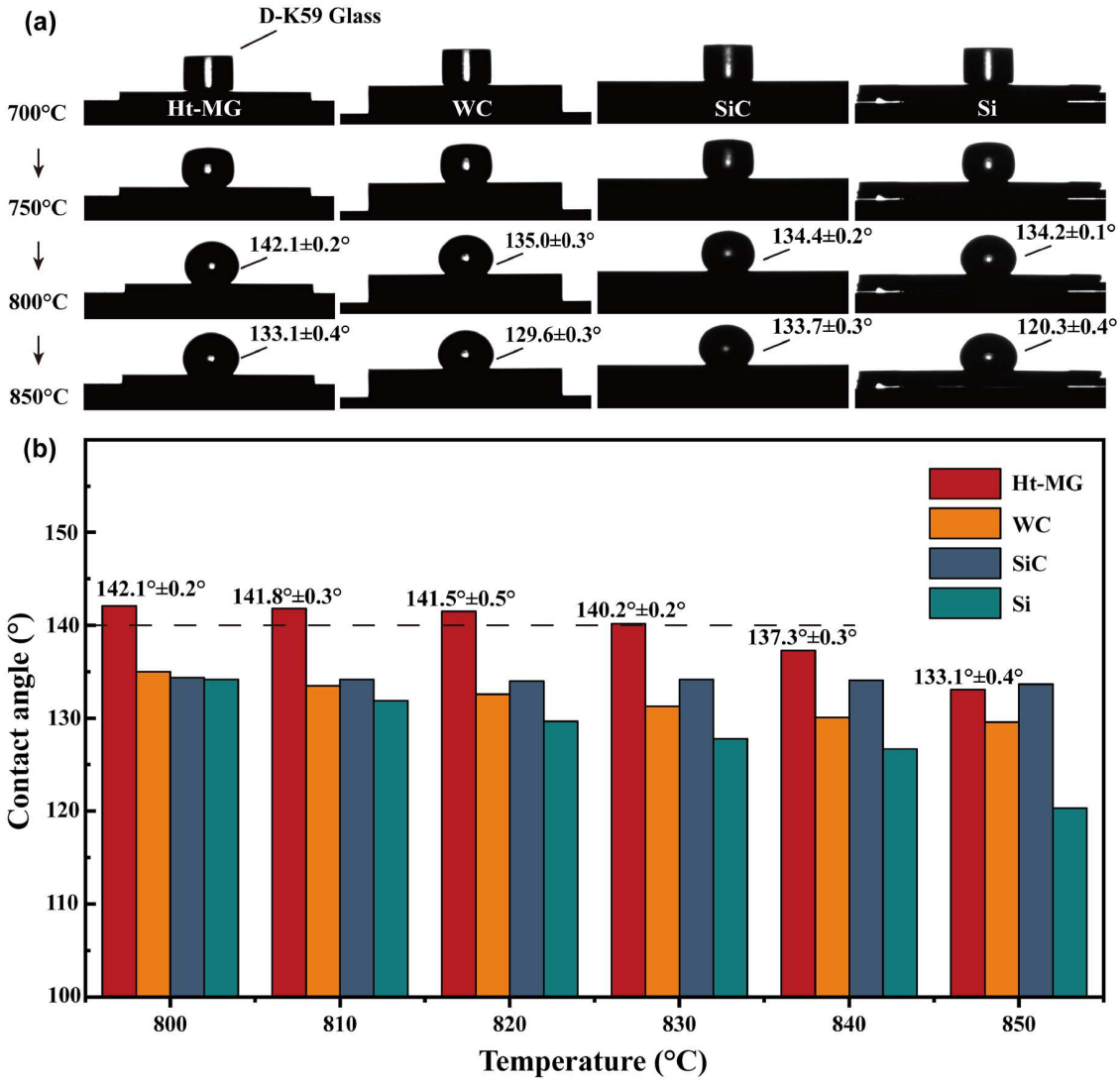

Figure 3 (Color online) (a) Evolution of the HCA during the heating process; (b) detailed statistics of HCA.

ht-MG and the fabrication of glass MLA using the ht-MG mold. As shown in Figure 5(a), the ht-MG mold is fabricated by replicating the structure of Si template via TPF. The Si template is coated with 500 nm-thick Si_3N_4 to increase durability. The ht-MG mold was obtained after etching the residual Si with 45% HF acid. The glass MLA is fabricated by transferring the structure of ht-MG mold via PGM. Figure 5(b) and (c) shows the SEM image and 3D morphology of the Si template after coating. The spacing between lens units is 150 μm and the surface of the structure is uniform and defect-free. The cross-sectional profile indicates that the lens unit has a height of 25 μm and a diameter of 80 μm (Figure 5(d)).

According to the thermodynamic properties of ht-MG, the forming temperature for ht-MG was set at 900°C. After reaching the desired temperature, a load of 200 N was applied and held for 1 min. The pressure was released only after cooling, arriving at the RT. This process successfully fabricated Ht-MG molds with a diameter of 10 mm, as illustrated in Figure S2. To fabricate MLA, we heat the glass billet and the ht-MG mold to 530°C and press them with a load of 200 N for 1 min. The fabricated glass MLA is shown in Figure S3. In more detail, Figure 6(a_1)–(a_3) presents the SEM image and 3D morphology of the ht-MG mold. It can be seen that the lens units exhibit excellent uniformity and no significant defects. Figure 6(a_3) demonstrates that the depth of the concave lens unit in ht-MG is 24.6 μm, which is consistent with the height of the lens unit in the Si template (approximately 25 μm), indicating that the MLA structure has been almost fully transferred to ht-MG with a replication rate of 98.4%. Correspondingly, Figures 6(b_1)–(b_3) presents the surface morphology of the glass MLA elements fabricated via the PGM process, which demonstrates the structural compatibility with the ht-MG molds. Notably, the

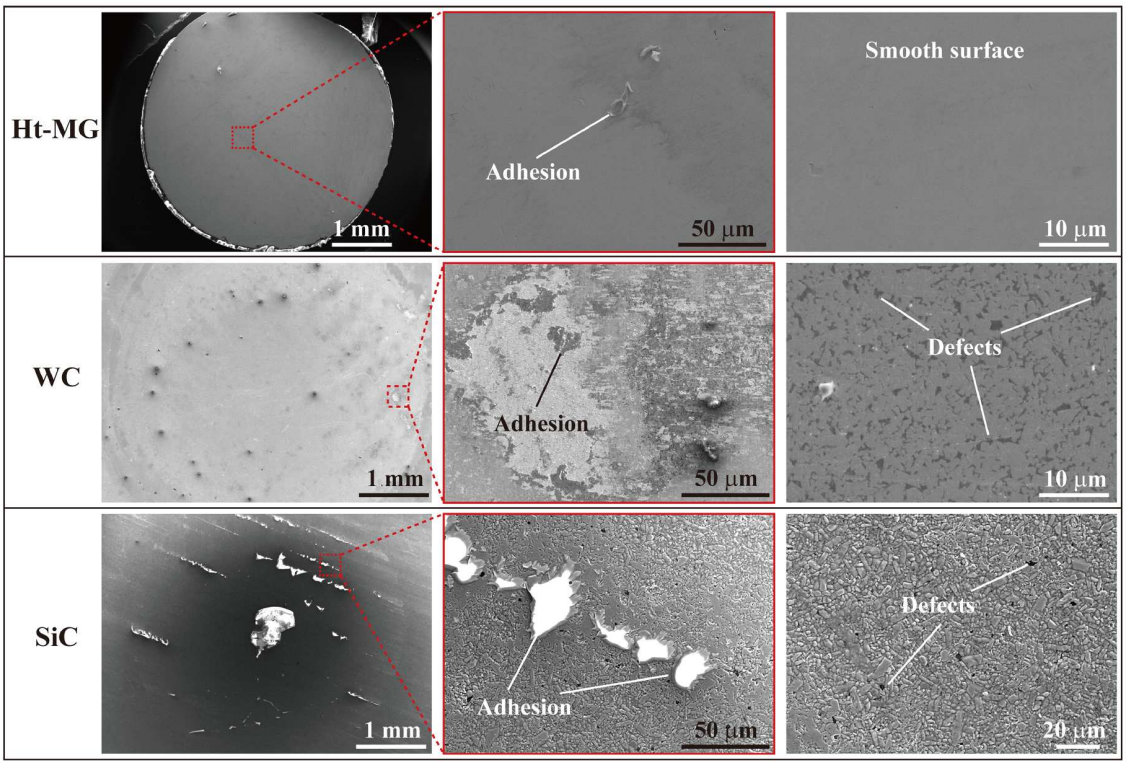

Figure 4 (Color online) Surface morphology of mold materials after 10 cycles of simulated PGM processing.

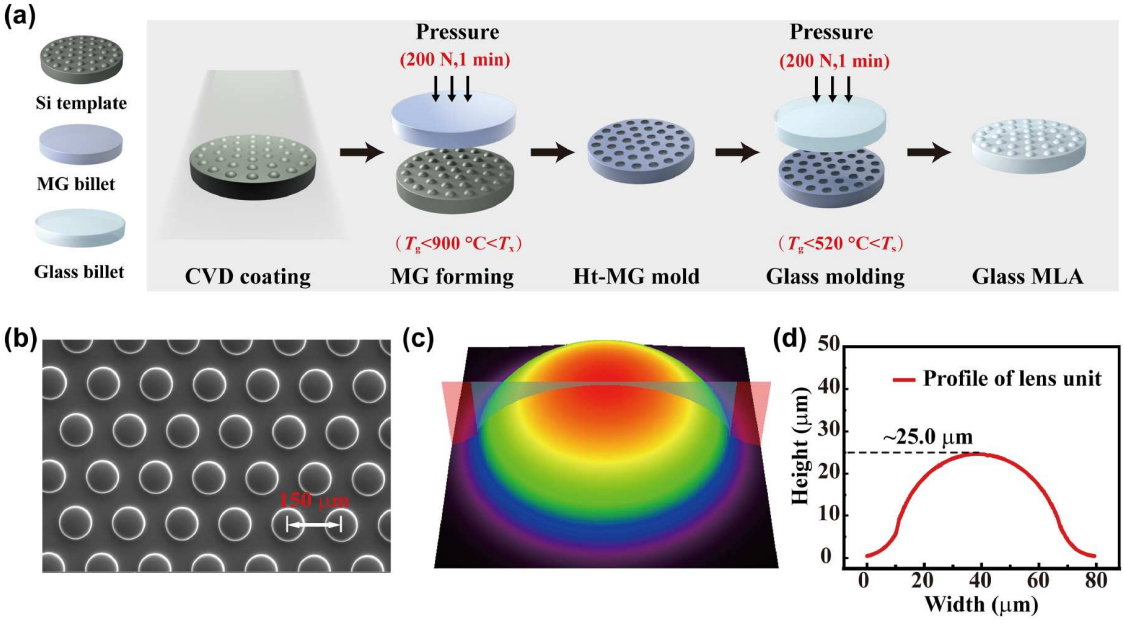

Figure 5 (Color online) (a) Schematic of the preparation process for ht-MG Molds and glass elements; (b) SEM morphology of Si template; (c) 3D morphology of the lens unit; (d) cross-sectional profile of the lens unit.

height of the lens unit on the glass is measured to be 24.5 μm, whereas the depth of the lens unit in the ht-MG mold is obtained as 24.6 μm, yielding a replication rate of 99.5% for the glass MLA fabricated via the ht-MG mold. In addition, Figure 6(c) compares the profiles of the lens unit in the Si template, the ht-MG mold, and the glass MLA element. It can be seen that the profile of the ht-MG mold is perfectly symmetrical with the Si template. Even after two consecutive

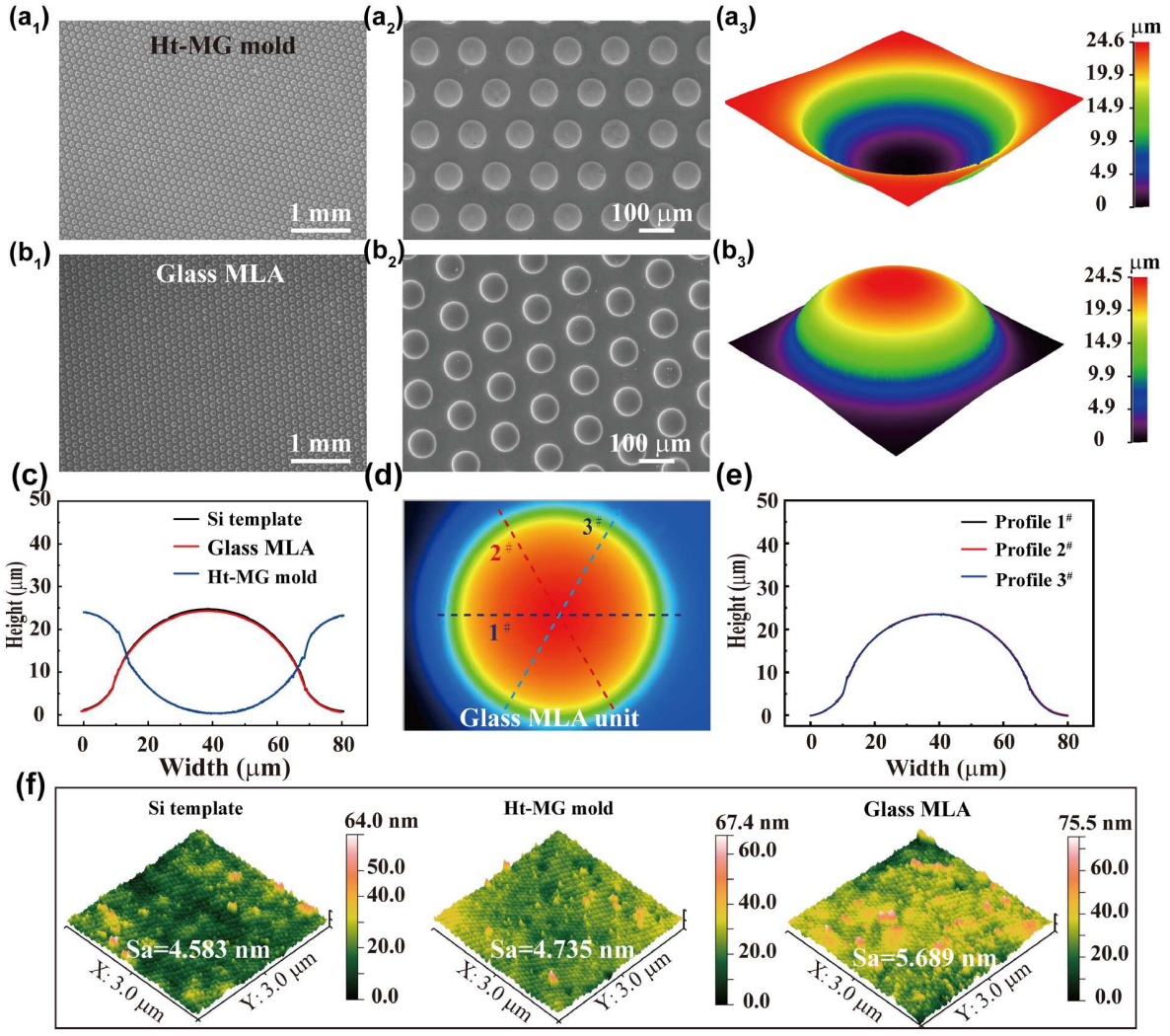

Figure 6 (Color online) (a_1)–(a_3) SEM images and corresponding 3D surface topographies of the ht-MG mold at different magnifications, showing well-defined microlens structures; (b_1)–(b_3) SEM images and 3D morphology of the replicated glass MLA at corresponding magnifications, demonstrating high-fidelity replication; (c) comparison of cross-sectional profiles of the MLA unit between the Si template, ht-MG mold, and glass product, highlighting the excellent shape transfer; (d), (e) cross-sectional profiles of a single glass MLA unit along two orthogonal orientations, indicating the isotropic nature of the molded features; (f) comparison of the surface roughness in representative regions of the Si template, ht-MG, and glass MLA (measured by atomic force microscopy).

transfer steps, the profile of the glass MLA lens unit nearly perfectly overlaps with the Si template, demonstrating a high-fidelity replication process. Moreover, the multi-directional center profiles of the final glass MLA elements were examined, as illustrated in Figures 6(d) and (e). The results indicate that the profiles of the glass lens units are perfectly coincident in three directions, which means that the glass lens units exhibit perfect symmetry and a well-defined spherical shape, ensuring that the MLA focal points remain in the same plane. The average surface roughness values of the Si template, ht-MG mold, and glass MLA components were also measured. As illustrated in Figure 6(d), the measurement area was selected at the top or bottom center of the lens unit within an area of 3 μm × 3 μm. As shown in Figure 6(f), the original Si template had an average surface roughness of 4.583 nm. After the TPF process, the surface roughness of the ht-MG mold increased slightly to 4.735 nm, indicating that the ht-MG mold largely retained the original smoothness of the Si template. The minimal increase in roughness indicates that no significant surface defects or roughness were introduced during the TPF process, ensuring high-fidelity structural replication. Furthermore, the average surface roughness of the glass MLA was measured at 5.689 nm, representing an increase of 1.106 nm compared with the original Si template. This result indicates that the usage of ht-MG as a mold effectively minimizes the loss of precision and maintains the surface quality close to that of the original template. Consequently, ht-MG molds provide a reliable solution for high-precision optical manufacturing and enable the fabrication of high-quality glass components.

3.4 Optical properties of glass MLA fabricated with ht-MG mold

Imaging performance is one of the key metrics for evaluating the optical quality of glass MLA. Figure 7(a) schematically illustrates the setup for the evaluation. A collimated light beam passes through a Z-shaped mask plate and forms a "Z" array in the focal plane after being focused by the glass MLA. The "Z" array is captured by a CCD camera equipped with a microscope head. The image shown in Figure 7(b) indicates that the "Z" letters are highly consistent without significant dispersion or distortion. This confirms that the fabricated glass MLA element exhibits excellent imaging performance.

Focusing ability is an alternative approach for evaluating the optical performance of glass MLA. Figure 8(a) schematically illustrates the setup for testing the focusing ability of the MLA. A collimated light beam emitted by an LED light source was directed perpendicularly onto a filter to obtain light of different wavelengths. The light passes through the filter and illuminates the glass MLA. A microscope objective lens is precisely adjusted to record the focused spots. The experimental results are displayed in Figure 8(b). The obtained spot arrays exhibit a uniform distribution of light intensity, indicating that the fabricated glass MLA possesses excellent focusing performance. Figure 8(c) shows the spot arrays at higher magnification. The obtained spots are fitted by two identical positive hexagons. It can be seen that the vertices of the hexagons are closely aligned with the spots. The edge of the inner hexagon is 150 μm long, and that of the outer hexagon is 300 μm. These lengths are consistent with the unit spacing of the ht-MG mold. This consistency confirms that the light passes through the glass MLA without deflection or distortion, demonstrating the reliable focusing performance. Furthermore, by introducing bandpass filters between the light source and the glass MLA, monochromatic light of various wavelengths including red light (~630 nm), orange light (~580 nm), and blue light (~470 nm) can be obtained (Figure 8(c)). Remarkably, the focusing performance remains excellent and is comparable to that of white light, confirming the general applicability of the fabricated glass MLA in the presence of various wavelengths.

4 Conclusion

In this work, high-fidelity microlens array (MLA) molds and glass components were successfully fabricated using an Ir-Ni-Ta-Nb high-temperature metallic glass (ht-MG) as the mold material. Through a thermoplastic forming process, MLA structures were precisely transferred to the ht-MG mold, achieving a replication rate of 98.4% and maintaining excellent structural fidelity. The fabricated ht-MG molds exhibited a low surface roughness (4.735 nm), only slightly higher than that of the original Si template, while the molded glass MLAs maintained high-quality optical surfaces with a roughness of 5.689 nm. Imaging and focusing experiments confirmed the excellent optical performance of the molded

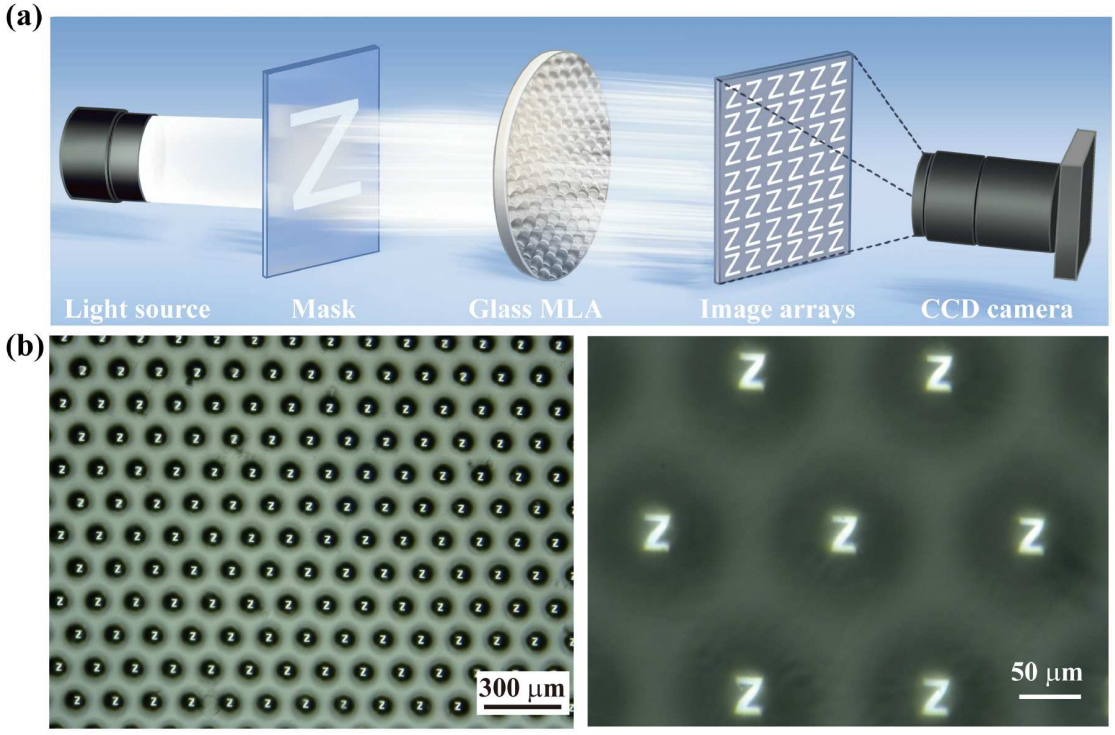

Figure 7 (Color online) (a) Schematic of the imaging experiment; (b) "Z" array image obtained by glass MLA.

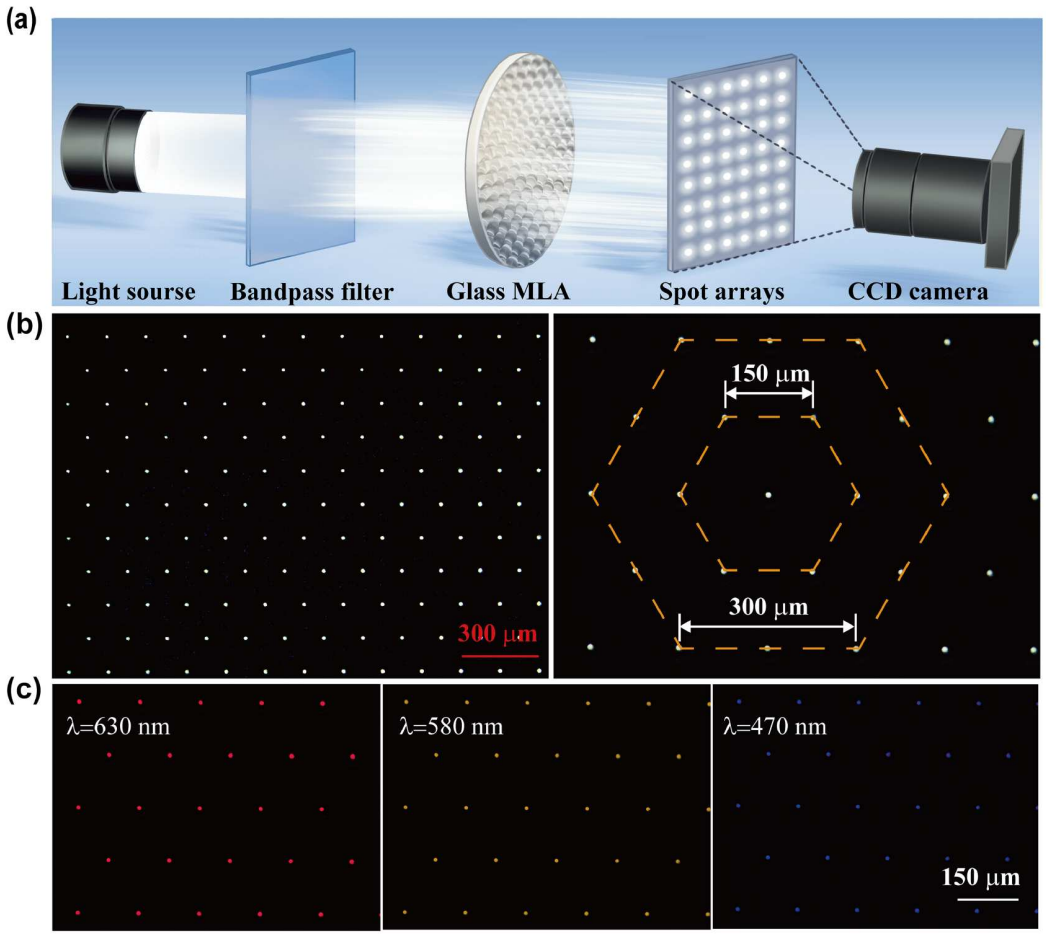

Figure 8 (Color online) (a) Schematic of the focusing experiment; (b) spot arrays obtained by MLA; (c) focusing results for light sources of different wavelengths.

glass MLAs, demonstrating precise light manipulation with minimal aberrations. These results verify that ht-MG molds enable reliable replication of high-precision optical structures and offer a scalable, effective approach for the production of high-performance glass optical components.

Acknowledgements This work was supported by the National Natural Science Foundation of China (Grant Nos. 52471070, 52402176), the Natural Science Foundation of Fujian Province (Grant No. 2024J08075), the Fujian University of Technology Foundation (Grant No. GY-Z24019), the Science and Technology Innovation Commission Shenzhen (Grant Nos. RCJC20221008092730037, 20220804091920001), and the Research Team Cultivation Program of Shenzhen University (Grant No. 2023QNT001).

Supporting Information The supporting information is available online at tech.scichina.com and link.springer.com. The supporting materials are published as submitted, without typesetting or editing. The responsibility for scientific accuracy and content remains entirely with the authors.

References

1 Zhang Q, Schambach M, Schlisske S, et al. Fabrication of microlens arrays with high quality and high fill factor by inkjet printing. Adv Opt Mater, 2022, 10: 2200677
2 Sun Z J, Liu Y Q, Wan J Y, et al. Reconfigurable microlens array enables tunable imaging based on shape memory polymers. ACS Appl Mater Interfaces, 2024, 16: 9581–9592
3 Ma Z, Hu X, Zhang Y, et al. Smart compound eyes enable tunable imaging. Adv Funct Mater, 2019, 29: 1903340–1903350
4 Yuan W, Li L H, Lee W B, et al. Fabrication of microlens array and its application: A review. Chin J Mech Eng, 2018, 31: 16
5 Choi M H, Han W, Min K, et al. Recent applications of optical elements in augmented and virtual reality displays: A review. ACS Appl Opt Mater, 2024, 2: 1247–1268
6 Li K, Huang X, Chen Q, et al. Flexible fabrication of optical glass micro-lens array by using contactless hot embossing process. J Manuf Process, 2020, 57: 469–476
7 Liu Y, Tong H, Li Y, et al. The effect of tool wear on the damaged layer thickness and tool wear rate in ultra-precision turning of quartz glass. J Micromech Microeng, 2023, 33: 095012
8 Gupta A, Saini A, Khatri N, et al. Review of single-point diamond turning process on IR optical materials. Mater Today-Proc, 2022, 69: 435–440
9 Bae S I, Kim K, Yang S, et al. Multifocal microlens arrays using multilayer photolithography. Opt Express, 2020, 28: 9082–9088
10 Xia Y, Jing X, Zhang D, et al. A comparative study of direct laser ablation and laser-induced plasma-assisted ablation on glass surface. Infrared Phys Tech, 2021, 115: 103737
11 Li P, Chen S, Dai H, et al. Recent advances in focused ion beam nanofabrication for nanostructures and devices: Fundamentals and applications. Nanoscale, 2021, 13: 1529–1565
12 Zhang L, Liu W. Precision glass molding: Toward an optimal fabri-

cation of optical lenses. Front Mech Eng, 2017, 12: 3–17
13 Ming W, Chen Z, Du J, et al. A comprehensive review of theory and technology of glass molding process. Int J Adv Manuf Technol, 2020, 107: 2671–2706
14 Zhang Y, Liang R, Spires O J, et al. Precision glass molding of diffractive optical elements with high surface quality. Opt Lett, 2020, 45: 6438
15 Zhou T, He Y, Wang T, et al. A review of the techniques for the mold manufacturing of micro/nanostructures for precision glass molding. Int J Extrem Manuf, 2021, 3: 042002
16 Sun S, Li K, Chu W, et al. Tungsten carbide molds for precision glass molding process: Mechanism of high-temperature degradation. Int J Refractory Met Hard Mater, 2022, 105: 105841
17 Zhou T, Xu R, Ruan B, et al. Fabrication of microlens array on 6H-SiC mold by an integrated microcutting-etching process. Precision Eng, 2018, 54: 314–320
18 Zhou T, Yan J, Liang Z, et al. Development of polycrystalline Ni-P mold by heat treatment for glass microgroove forming. Precision Eng, 2015, 39: 25–30
19 Mekaru H, Tsuchida T, Uegaki J, et al. Micro lens imprinted on Pyrex glass by using amorphous Ni-P alloy mold. Microelectron Eng, 2008, 85: 873–876
20 Holthusen A K, Riemer O, Schmütz J, et al. Mold machining and injection molding of diffractive microstructures. J Manuf Process, 2017, 26: 290–294
21 Klement Jun. W, Willens R H, Duwez P. Non-crystalline structure in solidified gold-silicon alloys. Nature, 1960, 187: 869–870
22 Inoue A, Takeuchi A. Recent development and application products of bulk glassy alloys. Acta Mater, 2011, 59: 2243–2267
23 Zhang Y, Sohrabi S, Li X, et al. Tailored gradient nanocrystallization in bulk metallic glass via ultrasonic vibrations. J Mater Sci Tech, 2025, 210: 109–120
24 Schroers J. The superplastic forming of bulk metallic glasses. JOM, 2005, 57: 35–39
25 Sohrabi S, Fu J, Li L, et al. Manufacturing of metallic glass components: Processes, structures and properties. Prog Mater Sci, 2024, 144: 101283
26 Li N, Chen Y, Jiang M Q, et al. A thermoplastic forming map of a Zr-based bulk metallic glass. Acta Mater, 2013, 61: 1921–1931
27 Liu J, Ruan W, Zhang H, et al. Highly efficient porous glass solar water evaporator. Adv Funct Mater, 2024, 35: 2415394
28 Sun F, Deng S, Fu J, et al. Superior high-temperature wear resistance of an Ir-Ta-Ni-Nb bulk metallic glass. J Mater Sci Tech, 2023, 158: 121–132
29 Li M X, Zhao S F, Lu Z, et al. High-temperature bulk metallic glasses developed by combinatorial methods. Nature, 2019, 569: 99–103
30 Wang C, Huang H, Qian Y, et al. One-step fabrication of regular hierarchical micro/nano-structures on glassy carbon by nanosecond pulsed laser irradiation. J Manuf Process, 2021, 62: 108–118
31 Roeder M, Guenther T, Zimmermann A. Review on fabrication technologies for optical mold inserts. Micromachines, 2019, 10: 233
32 Zhao H, Gain A K, Li Z, et al. Wear of mold surfaces: Interfacial adhesion in precision glass molding. Wear, 2023, 524–525: 204847
33 Zhou T, Wang Z, Ruan B, et al. Study on the blackening phenomenon of leaded glass during microgroove molding using nickel phosphorous mold. Ceramics Int, 2022, 48: 10420–10427
34 Halim Q, Mohamed N A N, Rejab M R M, et al. Metallic glass properties, processing method and development perspective: A review. Int J Adv Manuf Technol, 2021, 112: 1231–1258
35 Sun F, Yang J, Fu J, et al. Hierarchical macro to nano press molding of optical glasses by using metallic glasses. J Non-Crystalline Solids, 2022, 594: 121821
36 Zhang Y, Yan G, You K, et al. Study on α-Al_2O_3 anti-adhesion coating for molds in precision glass molding. Surf Coatings Tech, 2020, 391: 125720
37 Fischbach K D, Georgiadis K, Wang F, et al. Investigation of the effects of process parameters on the glass-to-mold sticking force during precision glass molding. Surf Coatings Tech, 2010, 205: 312–319
38 Zhao H, Zhang L, Gain A K, et al. Predicting the mold-glass interface adhesion in thermal molding. Int J Mech Sci, 2025, 294: 110265